

# Two-dimensional flow mapping past a circular cylinder using a 7-channel UDV system

Oleg Andreew<sup>1</sup> and André Thess<sup>2</sup>

<sup>1</sup> Helmholtz-Zentrum Dresden-Rossendorf, Bautzner Landstraße 400, 01328 Dresden, Germany

<sup>2</sup> Institute of Thermodynamics and Fluid Mechanics, Ilmenau University of Technology, P.O. Box 100565, 98684 Ilmenau, Germany.

A multichannel ultrasonic velocity profile (UVP) method has been applied for investigation of unsteady flow behind a circular cylinder. Using velocity profiles obtained by the ultrasonic velocimeter and their numerical post processing, two-dimensional time dependent flow maps were efficiently produced. A system of seven transducers immersed directly into the working fluid was used in order to simplify alignment of measurement lines and avoid the undesirable refraction of the acoustic beam on the walls. The von Kármán vortex street behind a cylinder were reconstructed as a pattern of large scale vortical flow.

**Keywords:** Flow around a cylinder, 2D flow mapping, multichannel UDV system

## 1 INTRODUCTION

According to the functioning principles of pulsed Doppler ultrasound velocimetry, a single transducer provides the projection of velocity vector along the direction of emitted acoustic beam. Two velocity components can be extracted from the UDV data when a measuring point is observed under at least two different angles. For example the authors [1] used a single movable transducer immersed directly into the working fluid in order to obtain a time-averaged plane velocity distribution in a liquid metal flow. A polynomial decomposition can be used for recalculation of acquired raw data into the 2D field of velocity vectors.

The purpose of the present work is to apply simultaneously 7 transducers for monitoring of unsteady time-dependent flow past a circular cylinder. Here the von Kármán vortex street which is characterized by the relatively large flow structures and low frequencies is used as an appropriate test object for application of multichannel UDV measuring system.

## 2 EXPERIMENTAL SETUP

### 2.1 Water channel

The experimental setup is shown in Figure 1. A circular cylinder ( $d=20$  mm in diameter) was dragged in a still water by a stepping linear motor with velocity varied in the range of  $U_0=10-30$  mm/s. The corresponding value of Reynolds number  $Re=U_0 d/\nu$  is  $Re=200-600$ . Here  $\nu=10^{-6}$  m<sup>2</sup>/sec is kinematic viscosity of water. Length, width and depth of the vessel were 700 mm, 300 mm and 50 mm correspondingly. We used a vessel filled with the water at rest in order to insure a homogeneous incoming velocity profile.

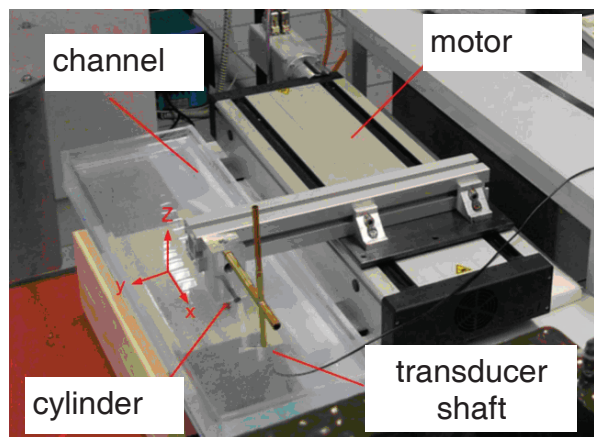


Figure 1: General view of experimental set up.

### 2.2 Measuring UDV system

We used a set of 7 transducers shown in Figure 2. The sound beams are adjusted in the horizontal plane situated on the half-depth of the vessel (25 mm). Angles of orientation of transducers with respect of the  $x$  direction are the following:  $\alpha_1=\alpha_2=360^\circ-45^\circ$ ,  $\alpha_3=360^\circ-30^\circ$ ,  $\alpha_4=0^\circ$ ,  $\alpha_5=30^\circ$ ,  $\alpha_6=\alpha_7=45^\circ$ . Diameters of transducers were 8 mm, operating frequency-8MHz. The transducers are acquired with the sampling rate of 50 ms by the multiplexer built in the DOP2000 system. The set of transducers was traveled at the distance of 150 mm behind the cylinder. For the flow mapping we recorded the data in the range between 15 and 135 mm along the ultrasound beam assuming that for every point the accuracy of the readings obtained from the different runs did not exceed 5% in relation to the bulk velocity. The estimated length of the "near field", where the acoustic field is nearly cylindrical, with a diameter slightly less than the diameter of emitter, is 47 mm. The half angle of the acoustic beam divergence for the "far field" is

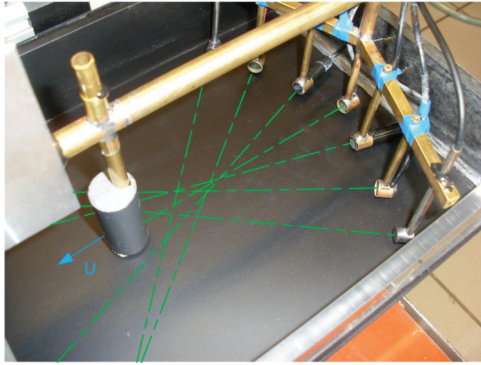
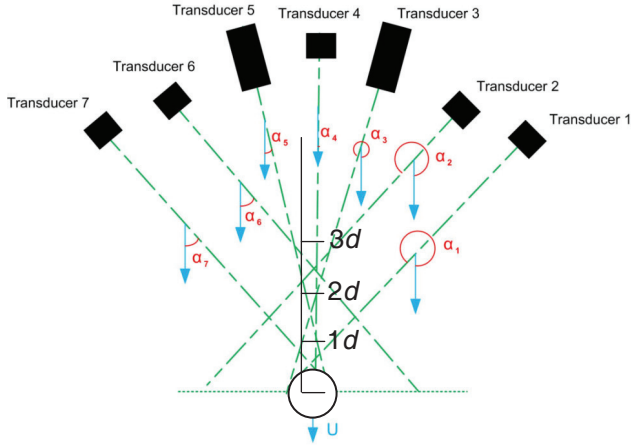


Figure 2: set of UDV transducers.

estimated to be  $2.96^{\circ} \pm 0.02^{\circ}$ . Thus, the beam diameter increases from 7-8 mm within the region of the “near field” to approximately 14-15 mm on the length of 120 mm from the surface of emitter. The spatial resolution of the method is defined by the mentioned diameters of the beam.

### 3 METHOD OF 2D FLOW MAPPING

#### 3.1 Principles of UDV

The UVP method is based on a pulsed ultrasound echography. The principles of UVP are broadly described in relevant publications (see, for example, [2]). Using the UVP method, the velocity profiles are recorded along a measuring line as a projection  $U$  of the true velocity vector  $\vec{V}$  onto the measuring line as shown in Figure 3(a) and defined by equation (1)

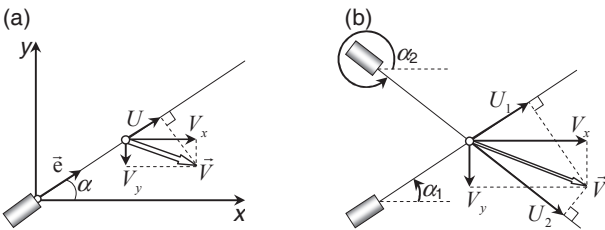


Figure 3: definition of velocity projection  $U$  measured by a UDV transducer.

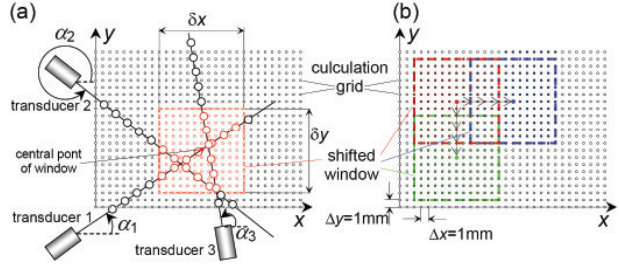


Figure 4: grid plane used for calculation of velocity components. (a) red color denotes the points of grid and UDV data used for polynomial decomposition within a current position of calculation window, (b) different position of the window and its central point.

$$U = \vec{V} \cdot \vec{e} = V_x \cos(\alpha) + V_y \sin(\alpha) \quad (1)$$

Here  $V_x$ ,  $V_y$  and  $\vec{e}$  are respectively the streamwise and spanwise components of velocity and the unit vector that defines the direction of the measuring line (angle  $\alpha$ ) with respect to the  $x$  axis. The projection  $U$  and the angle  $\alpha$  are the measured quantities. In order to calculate the true velocity vector, at least two measurement lines obtained under different angles  $\alpha_1 \neq \alpha_2$  must be used so that two velocity components can be calculated at the crossing points of measurement lines according to the following system of two linear equations:

$$\begin{cases} U_1 = V_x \cos(\alpha_1) + V_y \sin(\alpha_1) \\ U_2 = V_x \cos(\alpha_2) + V_y \sin(\alpha_2) \end{cases}$$

This procedure is illustrated in Figure 3(b).

#### 3.2 Two-D flow mapping

Practically it is not possible to identify precisely the position of the crossing points for the various sound beams. Moreover, the number of these points is not enough for a reliable flow mapping. For such a purpose we use all measurements points which lay within a small rectangular window as it illustrated in Figure 4(a). Here the red color identifies the points of a regular spatial grid used for velocity calculation and, also, the data from three transducers confined by the borders of the window.

For the flow mapping the stream- and spanwise velocity components,  $V_x(x,y)$ ,  $V_y(x,y)$  were approximated in the form of two-dimensional polynomial decomposition:

$$V_x(x,y) = \sum_{n=0}^4 \sum_{m=0}^4 u_{nm} \cdot P_{nm}(x,y), \quad V_y(x,y) = \sum_{n=0}^4 \sum_{m=0}^4 v_{nm} \cdot P_{nm}(x,y)$$

The polynomials  $P_{nm}(x,y)$  are defined as follows:

$$P_{nm}(x, y) = (x^n \cdot y^m)_{n+m \leq 4} = \begin{pmatrix} 1 & x & x^2 & x^3 & x^4 \\ y & xy & x^2y & x^3y & 0 \\ y^2 & xy^2 & x^2y^2 & 0 & 0 \\ y^3 & xy^3 & 0 & 0 & 0 \\ y^4 & 0 & 0 & 0 & 0 \end{pmatrix}$$

The coefficients  $u_{nm}$  and  $v_{nm}$  were calculated by solving the following system of linear equations:

$$\begin{pmatrix} \cos(\alpha_1) \sum_0^4 \sum_0^4 x_1^n y_1^m + \sin(\alpha_1) \sum_0^4 \sum_0^4 x_1^n y_1^m \\ \cos(\alpha_2) \sum_0^4 \sum_0^4 x_2^n y_2^m + \sin(\alpha_2) \sum_0^4 \sum_0^4 x_2^n y_2^m \\ \dots \\ \cos(\alpha_k) \sum_0^4 \sum_0^4 x_k^n y_k^m + \sin(\alpha_k) \sum_0^4 \sum_0^4 x_k^n y_k^m \end{pmatrix} \begin{pmatrix} u_{00} \\ \dots \\ u_{44} \\ v_{00} \\ \dots \\ v_{44} \end{pmatrix} = \begin{pmatrix} U_1 \\ U_2 \\ \dots \\ U_k \end{pmatrix} \quad (2)$$

Here  $k$  is the number of the data points measured within a rectangular window, whose centre corresponds to a calculating point (see Fig. 4). A pair of velocity components  $V_x(x, y)$ ,  $V_y(x, y)$  was calculated and associated with this central point according to the obtained coefficients  $u_{nm}$  and  $v_{nm}$ . These calculating points constituted a regular grid generated in the mid-plane of the channel with a 1 mm step in the spanwise streamwise directions. The vector  $(U_1, U_2, \dots, U_k)$  is the projection of velocity vectors obtained by the velocimeter for the data point with coordinates  $(x_1, y_1, x_2, y_2, \dots, x_k, y_k)$  observed by the transducer under the angles of  $(\alpha_1, \alpha_2, \dots, \alpha_k)$  in respect to the  $x$  axis. The data are distributed irregularly in the plane of measurement. The system (2) was solved by the standard solver for the linear least-squares problems implemented into the MatLab [3]. The size of the window was chosen as  $15 \times 15$  mm, the orders of polynomial decomposition were  $N = 4$  in streamwise and spanwise directions. This choice was a compromise in the order to ensure a well-posed system (2) and better spatial resolution of the data treatment procedure. The lower polynomial orders smooth the result, the higher ones give spurious extremes in velocity distribution.

## 4 RESULTS AND DISCUSSION

In Figure 5 we plot three flow patterns reconstructed by the described method for the flow past a circular cylinder at Reynolds number  $Re=500$ . In Figure 5(d) we show visualization for the same flow made by the small gas bubbles generated due to electrolysis on a thin tungsten wire. The wire was fed by the pulse electrical current. Duration of pulses and pauses was 2 sec. The flow behind a cylinder is an appropriate test object for our purpose. The von Kármán street is presented by a sequence of the large scale vortices. Dimensions of such vortices is commensurable with the diameter of the cylinder in the moment of generation and then increase in downstream direction. Reconstructed images in

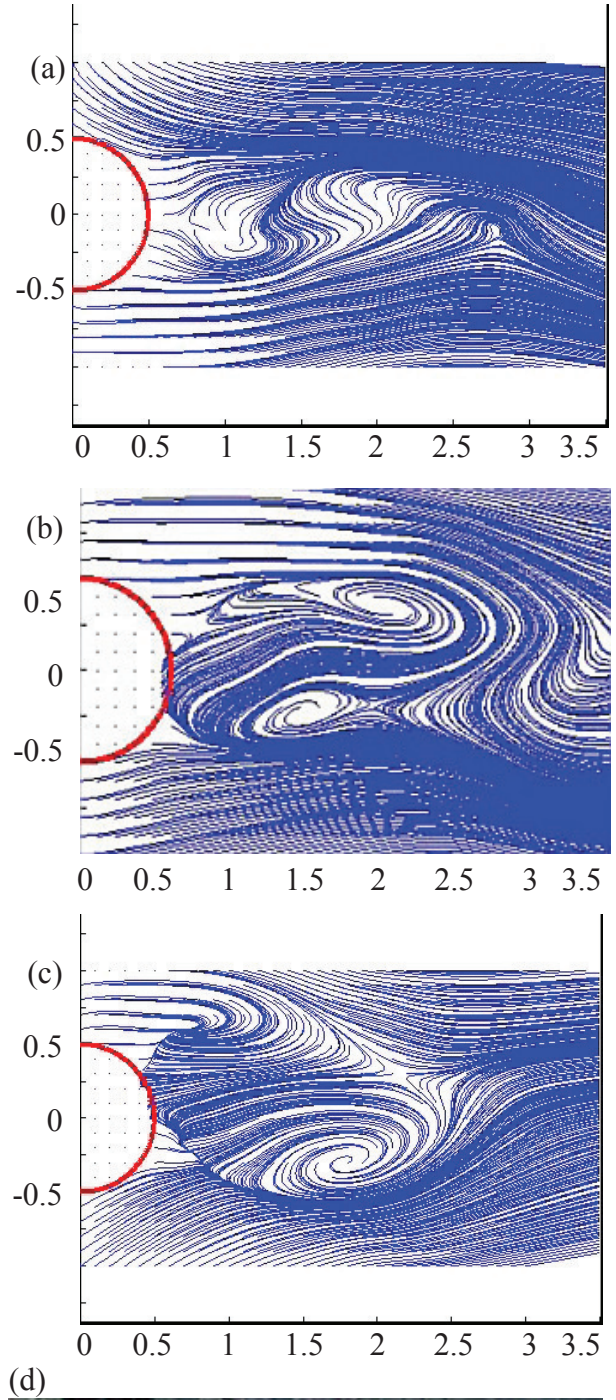


Figure 5: (a)-(c) snapshots of flow patterns reproduced according to the UDV data and (d) optical visualization of the flow behind the circular cylinder (von Kármán vortex street).  $Re=500$

Figures 5(a-b) present streamlines. Here we show snapshots of video file sampled with the rate of 20 frames per second. In general we managed to reproduce the pair of vortices on the distance of 2.5 gauges directly past the cylinder. According to Figure 2, this is the region which contains the data supplied by all seven transducers. In the transverse to the main flow  $y$ -direction the region of reliable flow reconstruction is restricted to one gauge of the cylinder. In spite of that the original flow (visualized in Figure 5(d)) is presented by the well pronounced vortices of the Kármán street, the applied method was not able to reproduce such flow structures continuously. Only 35% of the obtained by calculation frames contained the well developed vortices. The examples of successful frames are illustrated by images (b) and (c) in Figure 5. Unfortunately, the UDV data do not reproduce development of the vortex street in downstream direction. The region situated on the distance of 3-4 diameters of the cylinder is 'observed' by transducers number 3, 4 and 5 (see Figure 2). This is the region of so-called 'near field' of the ultrasound beam, where the transducers ensure the most reliable data. In spite of that, the method of flow mapping does not reproduce here the flow field reliably. That is definitely result of lack of data.

## CONCLUSIONS

The applied method of two-dimensional flow reconstruction is very exacting to plenitude of data. We managed to get the most reliable results in the flow regions where at least five transducers supplied the measurements under the different angles of observation. The time resolution was restricted approximately to 7 realistic frames per second at the acquisition rate of raw data 20 UDV profiles per second.

## ACKNOWLEDGMENTS

This work was supported by the Deutsche Forschungsgemeinschaft under contract number TH497/27-1.

## REFERENCES

- [1] Andreev, O., Kolesnikov, Yu., Thess, A. Application of the ultrasonic velocity profile method to the mapping of liquid metal flows under the influence of a non-uniform magnetic field, *Experiments in Fluids*, Volume 46, Number 1, January 2009, pp. 77-83(7)
- [2] Takeda Y; Kikura H (2002) Flow mapping of the mercury flow. *Exp Fluids* 32: 161-169
- [3] Coleman T; Li Y (1996) A Reflective Newton Method for Minimizing a Quadratic Function Subject to Bounds on Some of the Variables. *SIAM Journal on Optimization*, Vol. 6, Number 4: 1040-1058.